Mutations in the yeast two pore K^+ channel YKC1 identify functional differences between the pore domains

Paola Vergani[1], Michael R. Blatt*

[a] *Laboratory of Plant Physiology and Biophysics, University of London, Wye College, Wye, Kent TN25 5AH, UK*

Received 11 June 1999

Abstract **The K^+ channel of *Saccharomyces cerevisiae* encoded by the *YKC1* gene includes two pore-loop sequences that are thought to form the hydrophilic lining of the pore. Gating of the channel is promoted by membrane depolarisation and is regulated by the extracellular K^+ concentration ($[K^+]_o$) both in the yeast and when expressed in *Xenopus* oocytes. Our previous work showed that substitutions of equivalent residues L293 and A428 within the pore-loops had qualitatively similar effects on both the $[K^+]_o$-sensitivity of channel gating and its voltage-dependence. Here, we report that mutations of equivalent residues N275 and N410, N-terminal from the K^+ channel signature sequences of the two pores, have very different actions on channel gating and, in this case, are without effect on its voltage-sensitivity. The mutation N410D slowed current activation in a $[K^+]_o$-dependent manner and it accelerated deactivation, but without significant effect on the apparent affinity for K^+. The N275D mutant, by contrast, had little effect on the $[K^+]_o$-sensitivity for activation and it greatly altered the $[K^+]_o$-dependence of current deactivation. Neither mutant affected the voltage-dependence of the steady-state current nor the ability for other alkali cations to substitute for K^+ in regulating gating. The double mutant N410D-N275D showed characteristics of N410D in the $[K^+]_o$-sensitivity of current activation and of N275D in the $[K^+]_o$-sensitivity of deactivation, suggesting that little interaction occurs between pore domains with mutations at these sites. The results indicate that the two pore domains are not functionally equivalent and they suggest that the regulation of gating by external K^+ is mediated by K^+ binding at two physically distinct sites with different actions.**

Key words: Ion permeation; Site-directed mutagenesis; Outward rectifier K^+ channel; Potassium-dependent gating; *Saccharomyces cerevisiae*

1. Introduction

In contrast with animals, the cells of most plants and fungi maintain intracellular homeostasis and trans-membrane driving forces in widely differing ionic environments. These cells have evolved transport systems that are capable of sensing and responding to changing ionic gradients across the membrane to maintain the cellular homeostasis. The K^+ channels of many plant and fungal plasma membranes are a case in point, their gating being controlled by both membrane voltage and the extracellular K^+ concentration ($[K^+]_o$) [1–4]. However, until recently, no information has been available relating structural elements of any plant or fungal K^+ channel to these unusual $[K^+]_o$ and voltage-sensitivities.

The major K^+ outward rectifier of the yeast plasma membrane, encoded by the *YKC1* gene [5], is sensitive to both membrane voltage and to $[K^+]_o$ [1,2,6–8]. Sequence analyses have indicated that YKC1 contains eight trans-membrane spanning domains and two separate, conserved 'pore-loop' (P-loop) sequences, one linking trans-membrane domains 5 and 6 and the second linking trans-membrane domains 7 and 8, both thought to line the K^+ permeation pathway [2]. Sequence homology with other K^+ channels is restricted to the two P-loops [2,6,7]. The YKC1 sequence shows no evidence of a structural equivalent to the positively charged, S4 trans-membrane helix that contributes to voltage sensing of animal voltage-gated K^+ channels [9,10].

Sensitivities to both membrane voltage and $[K^+]_o$ are retained in the YKC1 gene product when expressed in *Xenopus* oocytes [2,6,8,11]. So, the major structural elements underlying these characteristics appear to be integral parts of the protein structure. In fact, single site mutations C-terminal to the GY(L)GD K^+ channel signature sequences of YKC1 have been shown to affect the dependence of gating on $[K^+]_o$, suggesting the presence of one or more regulatory K^+ binding sites near the outer mouth of the channel [11]. K^+ binding interacts with membrane voltage, if only because to occupy the site(s), the K^+ ion must traverse a large fraction of the membrane electric field [8]. It is not clear, however, whether K^+ binding occurs at more than one regulatory site, whether the voltage-sensitivity of the K^+ channel is necessarily coupled to K^+ binding and whether the two P-loops are similar in their contribution to the channel function.

The positions of the residues known to affect $[K^+]_o$-sensitivity in YKC1 correspond to the Shaker K^+ channel amino acid residue T449 which confers a $[K^+]_o$-dependence to C-type inactivation and is exposed to the outer surface of the membrane [12]. From comparisons with the recently solved structure of the KcsA K^+ channel [13], it appears that this residue may be closely juxtaposed to residues at the N-terminus of the pore helix. Of these, the residues N275 and N410 correspond to D431 in the Shaker K^+ channel which is also predicted to reside at the outer face of the membrane and, like T449, contributes to tetraethylammonium chloride (TEA) and toxin binding [14–16]. To better define the putative K^+ binding function of this domain and its relationship to YKC1 gating, we have substituted these asparagines and have characterised gating after expression of the mutant YKC1 channels in *Xenopus* oocytes. Here, we report that substitutions at these residues affect current relaxations at low $[K^+]_o$ without altering the voltage-dependence of gating and that the effects of the

*Corresponding author. Fax: (44) (1233) 813140.
E-mail: mblatt@wye.ac.uk

[1] Current address: Laboratory of Membrane Physiology, The Rockefeller University, 1230 York Avenue, New York 10021, USA.

0014-5793/99/$20.00
PII: S0014-5793(99)01167-9

same mutations, at the homologous positions within the two P-loops, are not equivalent.

2. Material and methods

2.1. Molecular biology

The pEXTM1 plasmid [8], containing the YKC1 open reading frame inserted between the 3′ and 5′ untranslated sequences of the *Xenopus* β-globin gene of the expression vector pBSXG1 [17], was used for mutagenesis, wild-type and mutant YKC1 channel expression. Mutagenesis was carried out by 'long primer' modification of the unique site elimination (USE) strategy [18] using a USE Mutagenesis kit (Pharmacia). The N410D-N275D and N275D-A428Y double mutant constructs were generated by inserting the *Bst*XI fragment containing a mutation in the second P-loop into plasmids previously mutagenised in the first P-loop. The N410D-A428Y double mutant was constructed on an A428Y template prepared using an alternate PCR strategy [19]. The accuracy of mutagenesis was checked in every case by sequencing on an ABI Prism310 DNA sequencer. Plasmids were linearised by digestion with *Hin*dIII and G(5′)ppp(5′)G-capped cRNA was synthesised using T7 polymerase (Cap-Scribe kit, Boehringer).

2.2. Electrophysiology

Stage V and VI oocytes were taken from mature *Xenopus laevis* and maintained at 18°C in a modified Barth's medium containing 88 mM NaCl, 1 mM KCl, 0.33 mM $Ca(NO_3)_2$, 0.41 mM $CaCl_2$, 0.82 $MgSO_4$, 2.4 mM Na_2CO_3, 0.1 mg/ml gentamycin sulfate and 80 U/ml penicillin. Oocytes were defolliculated manually using fire-polished Pasteur pipettes after partial digestion of the follicular cell layer by incubation for 1 h in modified Barth's medium with 2 mg/ml collagenase supplemented with 1 mg/ml trypsin inhibitor (Sigma). Defolliculated oocytes were injected with 1–30 ng cRNA in 30 nl water using a solid displacement injector (Drummond Nanoject, Drummond Scientific) and measurements were carried out 2–7 days post injection.

Macroscopic (whole-cell) current recordings were carried out under voltage clamp using an Axoclamp-2B (Axon Instruments) two electrode clamp circuit and virtual ground. Microprocessor interface was via a μLAB/μLAN analog/digital interface and software (WyeScience, Wye, Kent, UK). Intracellular microelectrodes were filled with 3 M KCl (input resistances <0.5 MΩ). Connection to the amplifier headstages was via a 3 M KCl/Ag-AgCl halfcell and matching halfcells with 3 M KCl-agar bridges were used for connection to the virtual ground. Measurements were carried out in a continuous flow of modified Ringer solution containing 100 mM (alkali chloride plus *N*-methylglucamine-Cl), 1 mM $MgCl_2$ and buffered with 5 mM HEPES titrated to pH 7.5 with $Ca(OH)_2$ ($[Ca^{2+}] \simeq 1$ mM). Data analysis was carried out using SigmaPlot (SPSS, Chicago, MI, USA) and the Marquardt-Levenberg algorithm [20].

3. Results

3.1. Equivalent mutations in the pore domains are dissimilar in their effects on activation

Macroscopic YKC1 current kinetics evoked upon depolarisation can be described by three distinct components. A near-instantaneous current appears within 1–2 ms (hereafter referred to as the 'instantaneous' component) and is followed by an exponentially relaxing component with a time constant of roughly 1 s (the 'fast' component) [2,8,21]. When the duration of the depolarisation is increased to >10 s, an additional component (the 'slow' component) is evident in low- and submillimolar $[K^+]_o$ [11]. These three current components are seen in Fig. 1A which shows currents recorded in wild-type YKC1-expressing *Xenopus* oocytes in response to 30 s steps to +50 mV from a holding voltage of −120 mV at four different $[K^+]_o$ values. Previous studies [8,11,22] demonstrated that the distribution between fast and slow components was sensitive to $[K^+]_o$ and this dependence is clearly evident here. In 0.1 mM $[K^+]_o$, the current is dominated by the slow component, the amplitude of which decreases with increasing $[K^+]_o$ and is virtually undetectable in 10 mM $[K^+]_o$.

We found that substituting the asparagine at position 410 in the second P-loop with an aspartate residue had a dramatic effect on the kinetics of activation at low $[K^+]_o$. Fig. 1C shows a family of relaxation curves in an oocyte expressing the N410D mutant YKC1 channel. By comparison with the wild-type current (Fig. 1A), the mutant showed little instantaneous component and rose with a slow, sigmoidal time course in 0.1 mM $[K^+]_o$. Increasing $[K^+]_o$ accelerated the overall activation and, in addition, progressively reduced the sigmoidal character so that in 10 mM $[K^+]_o$, wild-type and N410D current relaxations were virtually indistinguishable.

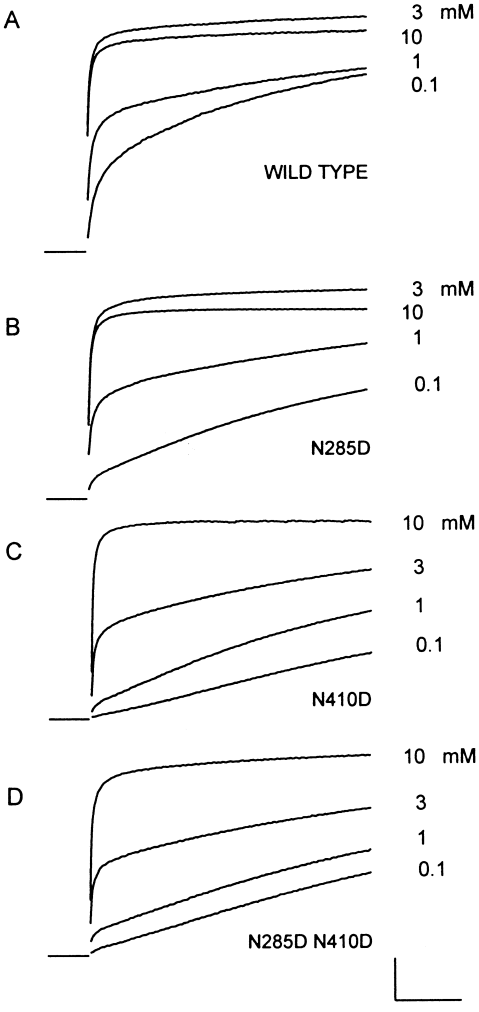

Fig. 1. Mutations slow the voltage-dependent activation of the YKC1 K^+ channel at low $[K^+]_o$. Families of current trajectories from representative oocytes expressing wild-type (A) and the mutants N275D (B), N410D (C) and N410D-N275D (D). Data recorded in $[K^+]_o$ from 0.1 to 10 mM upon stepping membrane voltage to +50 mV for 60 s following a 10 s conditioning step to −120 mV. Voltage steps in 0.1–1.0 mM $[K^+]_o$ were of 60 s duration although only 30 s are shown. The external K^+ concentration is indicated (right). Zero current level is indicated by each set of traces (left). Scale: vertical, 10 μA; horizontal, 5 s.

Other amino acids, tyrosine, serine and alanine, were substituted for N410. However, all failed to give a measurable current after injections of the cRNA in *Xenopus* oocytes.

Mutation of the equivalent residue in the first P-loop, that is the asparagine at position 285, also influenced the kinetics of activation, but the effect was less severe. Fig. 1B shows a family of relaxation curves in an oocyte expressing the N275D mutant YKC1 channel. In this case, the mutant showed a reduced instantaneous component but no sigmoidal time course at any $[K^+]_o$. Again, increasing $[K^+]_o$ accelerated the overall activation to give current relaxations that were indistinguishable from the wild-type in 10 mM $[K^+]_o$. To explore possible interactions between mutations within and between the two P-loops, we constructed the double mutants N410D-N275D, N275D-A428Y and N410D-A428Y. Of these constructs, only the N410D-N275D mutant gave a measurable current when expressed in oocytes. Currents carried by this mutant were visually indistinguishable from N410D currents (Fig. 1D, but see below).

3.2. Mutation N410D affects the sensitivity of current activation kinetics to $[K^+]_o$

Overall, the mutations N410D and to a lesser extent N275D affected activation kinetics so that at low $[K^+]_o$, activation of the mutant was slowed by comparison with the wild-type. We found that increasing $[K^+]_o$ accelerated activation by affecting the distribution of current among kinetic components, as illustrated in Fig. 2. The time courses for the activation of wild-type and mutant currents were described as the sum of a constant term plus two exponentials corresponding to the instantaneous, fast and slow components, respectively. So,

$$I/I_{max} = a_i + a_f(1-e^{-k_f t}) + a_s(1-e^{-k_s t}) \quad (1)$$

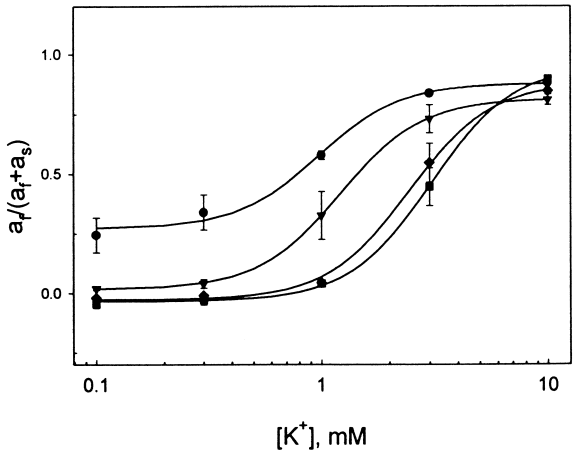

Fig. 2. Mutation in the second P-loop, but not in the first, reduces the sensitivity of YKC1 current activation to extracellular K^+. The amplitude of the fast component, relative to the total amplitude of the time-dependent current components ($a_f/(a_f+a_s)$), plotted as a function of $[K^+]_o$. Data are means ± S.E.M. of (n) independent experiments for wild-type (●, $n=6$) and mutants N275D (▼, $n=4$), N410D (■, $n=4$) and N410D-N275D (♦, $n=3$). Amplitudes were determined by fitting sets of current relaxations (see Fig. 1) to Eq. 1. Curves (solid lines) are best fits to the Hill equation (Eq. 2) with a common Hill coefficient of 2.4 ± 0.3. Fitted parameters, y_0, y_{max}, $K_{1/2}$, respectively: wild-type, 0.27 ± 0.02, 0.61 ± 0.03, 1.0 ± 0.1 mM; N275D, 0.02 ± 0.02, 0.81 ± 0.03, 1.2 ± 0.2 mM; N410D, −0.03 ± 0.01, 0.98 ± 0.03, 3.1 ± 0.2 mM; N275D-N410D, −0.03 ± 0.01, 0.91 ± 0.03, 2.6 ± 0.3 mM.

where a_i, a_f and a_s are the amplitudes of the instantaneous, fast and slow components and k_f and k_s are the corresponding rate constants. Parameters obtained from fittings of the wild-type [11] showed that a major effect of increasing $[K^+]_o$ was to decrease the amplitude of the slow component relative to the other kinetic components. Thus, increasing $[K^+]_o$ accelerated the overall time course of activation by favouring the other, faster, components. We therefore used the relative amplitudes of the time-dependent components obtained from fittings to

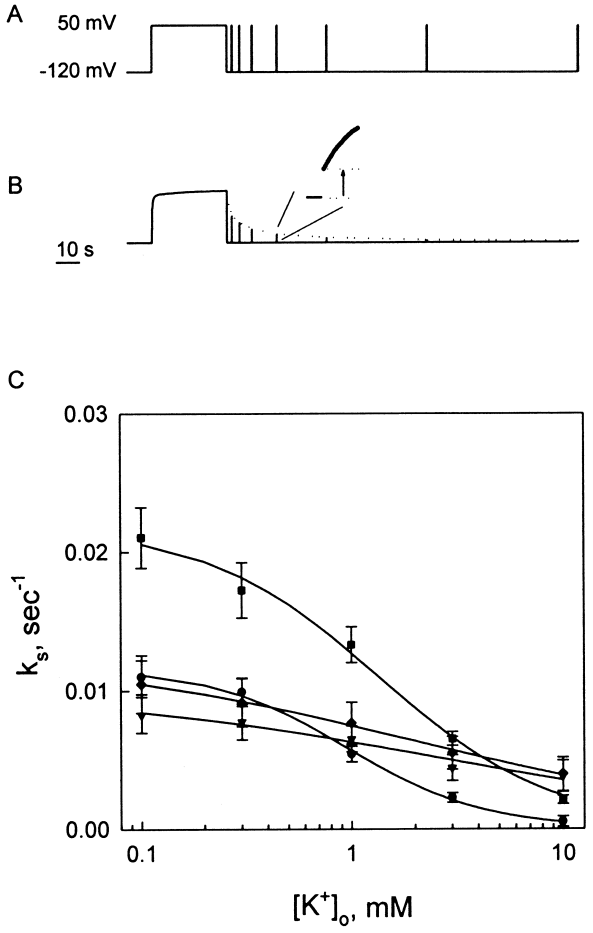

Fig. 3. Mutation in the first P-loop, but not in the second, affects the $[K^+]_o$-sensitivity of YKC1 deactivation kinetics. Transit into distal closed states was measured as the rate of escape from instantaneous reactivation using a multiple-step protocol shown in (A). Representative current trace (B) with expanded current relaxation during step return to +50 mV (inset) showing the amplitude of the 'instantaneous 'current measured at 10 ms from the start of the test pulse. After normalising to the current value measured at the end of the 30 s activating step ($I_{inst,rel}$), this amplitude was used to derive the fraction of instantaneously activatable current as a function of the interpulse duration from fitting to Eq. 3 (B, dotted line). (C) Effect of $[K^+]_o$ on k_s plotted as the mean rate constant ± S.E.M. of (n) independent experiments for wild-type (●, $n=6$) and mutants N275D (▼, $n=3$), N410D (■, $n=4$) and N410D-N275D (♦, $n=3$). Solid lines are the results of fittings to a logistic function (Eq. 4) where $K_{1/2}$ is the $[K^+]_o$ at which k_s dropped to half of the maximal value R. Fitted parameters R, n, respectively: wild-type, 0.0117 ± 0.0008 s^{-1}, 1.2 ± 0.3; N275D, 0.0101 ± 0.0026, 0.5 ± 0.2; N410D, 0.0219 ± 0.0009, 1.0 ± 0.1; N275D-N410D, 0.0127 ± 0.0026, 0.5 ± 0.2. $K_{1/2}$ values given in the text.

construct dose-response curves (Fig. 2). The data were well-fitted to the Hill equation

$$y = y_0 + y_{max}\frac{[K^+]^n}{K_{1/2}^n + [K^+]^n} \quad (2)$$

where y is the relative amplitude of the fast component ($=a_f/(a_f+a_s)$). Joint fittings of the means yielded a common cooperativity coefficient, n, of 2.4 ± 0.3 (Fig. 2, solid lines). For both wild-type and mutant channels, the relative amplitude of the fast component rose with $[K^+]_o$ in a dose-dependent fashion. For the N275D mutant, the larger fraction of current in the slow component was reflected in the near-zero value of the ratio at low $[K^+]_o$. For the N410D mutant of the second P-loop, the slower activation and the sigmoidicity of the current trajectory at the lowest $[K^+]_o$ gave negative values for a_s and, thus, a negative value for the ratio at this concentration. Fittings yielded statistically equivalent values for $K_{1/2}$ in the wild-type and N275D mutant YKC1 channels (means ± S.E.M. (n): wild-type, $K_{1/2} = 1.0 \pm 0.1$ mM (6); N275D, $K_{1/2} = 1.2 \pm 0.2$ mM (4)). The effect of the N410D mutation in the second P-loop was much more pronounced and gave a significantly higher value for $K_{1/2}$ (mean ± S.E.M., 3.1 ± 0.2 (4)). The characteristics of the double mutant N410D-N275D were similar to the single N410D mutant and gave a value for $K_{1/2}$ of 2.6 ± 0.3 (3). Thus, the effect of mutation on the current kinetics was marked by a decrease in the apparent affinity for K^+ for the N410D and double mutants, but not for the N275D mutant.

3.3. Mutation N275D affects the sensitivity of current deactivation kinetics to $[K^+]_o$

Closing of the YKC1 K^+ channels upon re-polarisation of the membrane occurs within 1–2 ms and has been associated with entry into the proximal closed state [2,8]. Therefore, tail currents could not be resolved satisfactorily for detailed kinetic analysis. Instead, to investigate the effect of the mutations on the slower events of deactivation, we used a multiple pulse protocol, varying the interpulse intervals. The current was activated with 30 s steps to +50 mV and the voltage then stepped to −120 mV for varying lengths of time (Fig. 3A). The channel population remaining in the instantaneously activatable pool at the end of this variable period was then assayed 10 ms into a second step to +50 mV and the current was normalised to the steady-state current recorded at the end of the first 30 s step. Because transitions between the open state and the immediate closed state are virtually instantaneous [2,8], this manipulation gives a measure of the rate of escape from the immediate closed state to more distal closed states [11].

The example in Fig. 3B shows one set of measurements using this protocol. The current fraction reactivated 'instantaneously' as a function of the interpulse duration reflects the time course of relaxation (dotted line) into more distal closed states from which only time-dependent reactivation was possible. Each set of data was well-described by the sum of two falling exponentials without offset, such that

$$I_{inst,rel} = a_{df}e^{-k_f t} + a_{ds}e^{-k_s t} \quad (3)$$

where a_{df} and a_{ds} are the (relative) amplitudes of the two components of deactivation. The rate constant of the slowest

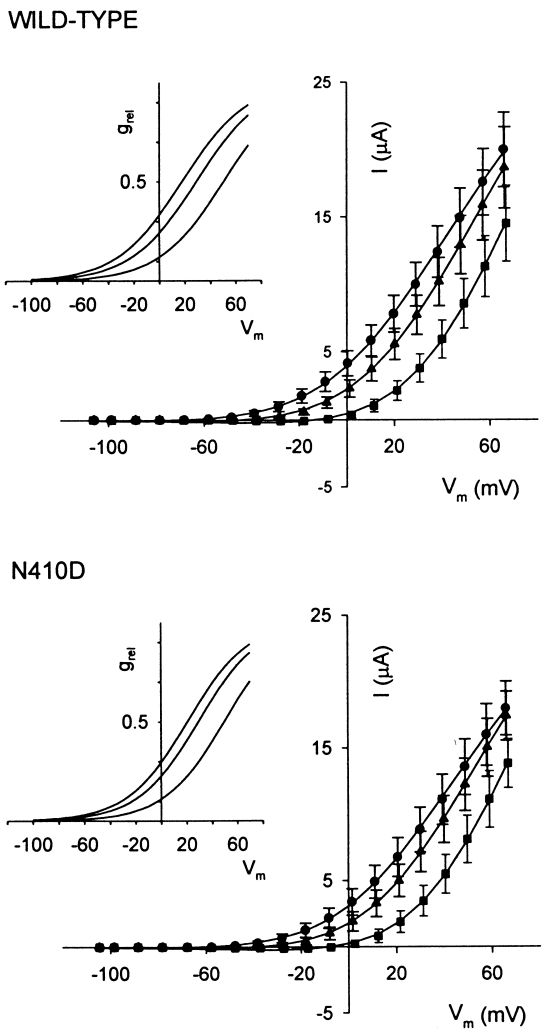

Fig. 4. Mutations have no effect on the $[K^+]_o$-sensitivity of the steady-state current-voltage relations. Currents from oocytes expressing the YKC1 wild-type (top) and the N410D mutant (bottom) channel measured in 10(●), 30(▲) and 100 mM (■) $[K^+]_o$ fitted jointly to a Boltzmann function (Eq. 5, solid lines). Data are means ± S.E.M. from 12 (wild-type) and nine (N410D) oocytes. Insets show the corresponding g_{rel}-voltage curves derived from the fitted current-voltage curves (see [8]). Fitted parameters (wild-type): $V_{1/2}$, +18 ± 1 mV (10 mM), +29 ± 1 mV (30 mM), +50 ± 2 mV (100 mM $[K^+]_o$); $[K^+]_i$, 157 ± 9 mM. Parameter values for the mutants did not differ significantly from these.

component, k_s, decreased as $[K^+]_o$ was increased in every case, while k_f was largely independent of $[K^+]_o$ (not shown). Values of the rate constant for the slowest component were well-fitted to a logistic (dose-response) function

$$k_s = \frac{R}{1 + \frac{[K^+]_o}{K_{1/2}}} \quad (4)$$

where $K_{1/2}$ is the $[K^+]_o$ at which k_s drops to half its maximal predicted value R. For the wild-type YKC1 current (solid circles), the fitting shown in Fig. 3C yielded $K_{1/2} = 1.0 \pm 0.2$ mM ($n = 6$). The N410D mutant (solid squares) showed a roughly 2-fold enhancement in the rate of deactivation at all values of $[K^+]_o$. No significant difference was evident in k_f

between the mutant and wild-type (not shown). Again, values for k_s were well-fitted to the logistic function (Eq. 4) and gave fitted parameters for N410D of $K_{1/2} = 1.4 \pm 0.2$ mM ($n = 4$).

By contrast, the N275D mutant (solid triangles) exhibited a 'flattened' response of k_s to $[K^+]_o$ (Fig. 3C). Again, values for k_f showed no significant difference from the wild-type (not shown) and, at submillimolar $[K^+]_o$, current relaxations of N275D were similar to the wild-type. However, in 10 mM $[K^+]_o$, the rates of escape from the instantaneously activated pool remained high compared to the wild-type. Unexpectedly, similar results were obtained with the double mutant N410D-N275D (solid diamonds). The range of our measurements does not allow for accurate estimation of $K_{1/2}$ in these instances. Nonetheless, the data could be fitted to Eq. 4, yielding values of $K_{1/2}$ near 3 mM and values for n of 0.5 ± 0.2 for both mutants, suggesting a negative cooperativity for K^+ binding. Thus, in general, increasing $[K^+]_o$ appeared to slow the rate of transitions out of the open state into the more distal closed states of the channel. The N410D mutant showed an accelerated rate of deactivation and had a small, but not very significant effect on the apparent affinity for K^+. The N275D mutant and the double N410D-N275D mutant each showed a profoundly reduced sensitivity of the channels to K^+ in its action on deactivation.

3.4. Mutation has no effect on the voltage and cation-sensitivity of the steady-state conductance

Because the mutations N410D and N275D altered activation and deactivation in a complementary fashion, the effect might have been expected to show in the voltage-dependence of the relative steady-state conductance. In general, the effects on activation or deactivation could be seen to favour more distal closed states of the channel by slowing exit from these states on depolarisation while speeding return to the same states on re-polarisation. However, we found that current-voltage (I-V) curves for the N410D, N275D and the double mutant were not displaced to more positive voltages relative to the wild-type YKC1 current characteristics. Fig. 4 shows the I-V characteristics for wild-type and the N410D mutant at 10, 30 and 100 mM $[K^+]_o$. The corresponding relative conductance-voltage (g_{rel}-V) curves (Fig. 4, insets) were derived from joint fittings of the data at the three $[K^+]_o$ to a Boltzmann function of the form

$$I = \frac{g_{max}(V - E_K)}{1 + e^{\delta F(V - V_{1/2})/RT}} \quad (5)$$

and then normalised to the predicted conductance maximum g_{max}. Here, δ is the voltage-sensitivity coefficient for channel activation, $V_{1/2}$ is the voltage giving half-maximal activation and E_K, F, R and T have their usual meanings.

Current-voltage (I-V) curves for the wild-type showed the characteristic outward rectification of YKC1 and shift towards more positive potentials as $[K^+]_o$ was increased from 10 mM to 30 and 100 mM. For N410D as for the wild-type YKC1 current over this concentration range, the relative conductance was displaced in parallel with E_K (see Fig. 4, insets) and the voltage-dependence for channel opening was unaffected by the mutation, as determined by the Boltzmann voltage-sensitivity coefficient δ. Also, a comparison of the half-maximal activation voltages (Fig. 5) showed that neither of the two single mutants nor the N410D-N275D double mutant

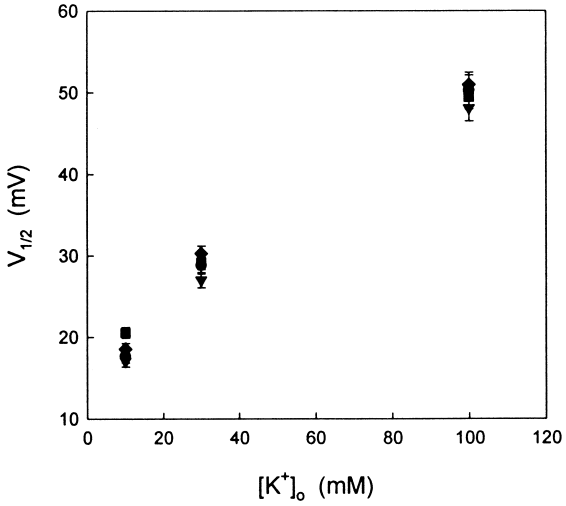

Fig. 5. Mutations have no effect on the interaction of voltage with the $[K^+]_o$-sensitivity of the steady-state current-voltage relations. Mean values ± S.E.M. for $V_{1/2}$ derived from fittings to Eq. 5, including those in Fig. 4, plotted as a function of $[K^+]_o$ for wild-type (●, $n = 12$) and mutants N275D (▼, $n = 9$), N410D (■, $n = 8$) and N410D-N275D (◆, $n = 4$).

displaced values for $V_{1/2}$ significantly relative to the wild-type.

Previous studies had shown that Rb^+ and Cs^+, like K^+, affected the voltage-sensitivity of the wild-type YKC1 current in the steady-state [8]. We therefore also compared the voltage-sensitivities of the wild-type, N410D and N275D mutant currents in Rb^+ and Cs^+. The values for $V_{1/2}$ were determined from steady-state current-voltage data as before, but recorded in 10 mM Rb^+ and Cs^+ as substitutes for K^+. For the wild-type, values for $V_{1/2}$ in 10 mM $[Rb^+]_o$ and 10 mM $[Cs^+]_o$ were displaced $+14 \pm 2$ mV and $+9 \pm 2$ mV, respectively, relative to 10 mM $[K^+]_o$. Virtually the same results were obtained for the N275D mutant and for the N410D mutant, the relative displacements were $+18 \pm 3$ mV for 10 mM $[Rb^+]_o$ and $+14 \pm 2$ mV for 10 mM $[Cs^+]_o$. Thus, neither mutant affected the alkali cation specificity evident in the voltage-dependence of gating.

4. Discussion

Activation of the YKC1 K^+ channel of yeast, like that of many K^+ channels in plants [3,4,23], is gated both by membrane voltage and by the external K^+ concentration. Channel opening is favoured by membrane depolarisation and is suppressed by increasing $[K^+]_o$ so that further depolarisation is necessary to achieve the same relative conductance. These observations have raised questions about the features of the channel protein that are responsible for its K^+ and voltage-sensitivities. Our previous work identified a pair of corresponding residues, one in each of the P-loops, that affected both the $[K^+]_o$-sensitivity of the channel and its interaction with voltage [11]. These residues were situated C-terminal from the GY(L)GD K^+ channel signature sequences. The present study defines additional positions within the pore structures that contribute to the $[K^+]_o$-dependence of the channel. We find (1) that the N410D point mutation in the second P-loop causes a slowing of activation kinetics and faster deactivation, (2) that the same mutation at the equiv-

alent position in the first P-loop has a less severe effect on activation, but very different effects on deactivation, (3) that both mutations alter the apparent $K_{1/2}$ for $[K^+]_o$ action, for N410D in activation and for N275D in deactivation, but that neither leads to a shift in the steady-state voltage-dependence of the current or its specificity among alkali cations and (4) that the N410D-N275D double mutant shows a sum of characteristics of each single mutation with respect to the $[K^+]_o$-sensitivity of the channel. These results indicate a functional asymmetry between the two P-loops. They also suggest the existence of two separate K^+ binding sites that regulate channel gating, only one of which modulates the steady-state voltage-dependence of the current.

The antiparallel effects of the N410D and N275D mutations on the kinetics for activation and deactivation are consistent with serial models for YKC1 channel gating that have been proposed before [2,8,11,21]. Previous analysis of the $[K^+]_o$-dependence of gating indicated a serial four state model to account for the slow kinetic components:

$$C_4 \underset{k_{43}}{\overset{k_{34}}{\leftrightharpoons}} C_3 \underset{k_{32}}{\overset{k_{23}}{\leftrightharpoons}} C_2 \underset{k_{21}}{\overset{k_{12}}{\leftrightharpoons}} O_1 \qquad [S1]$$

According to this model, the most distal closed state (C_4) is connected to the others by a very slow transition (rate constants k_{43} and k_{34}) and the channel must pass sequentially through two further closed states (C_3 and C_2) before reaching the open state (O_1). Transit between C_2 and O_1 is virtually instantaneous while fast activation ($\tau \sim 1$ s) is associated with transit out of the more distal closed state C_3 [2,8]. Thus, the relative occupancy of each of these states immediately preceding a positive voltage step determines the relative amplitude of the instantaneous, fast and slow components to current activation.

We had shown [8,11] that increasing $[K^+]_o$ has two distinct effects. First, it accelerated activation by reducing the relative contribution of the slow component and delayed exit from the instantaneously activatable pool by reducing the slow relaxation rate constant in channel deactivation. These effects were seen at sub- and low-millimolar $[K^+]_o$, consistent with a binding site with an apparent $K_{1/2}$ near 1 mM. Second, raising $[K^+]_o$ reduced the steady-state conductance at any one voltage so that the conductance was displaced in parallel with E_K along the voltage axis. These effects were seen at $[K^+]_o$ values near 10 mM and above. At 1–3 mM $[K^+]_o$ and below, no further $[K^+]_o$-dependence was measurable in steady-state conductance. Thus, in context of the serial model S1, both $C_4 \leftrightharpoons C_3$ and $C_3 \leftrightharpoons C_2$ transitions appeared to be affected by $[K^+]_o$, but over two distinct concentration ranges, suggesting that K^+ bound at two different sites. At low $[K^+]_o$, binding to the high-affinity site could be seen to stabilise the conformation corresponding to the C_3 state, drawing channels out of the C_4 state. At higher $[K^+]_o$, binding to the lower affinity site would stabilise the C_3 with respect to the C_2 (and O_1) state. Mutation of A428 in the second P-loop and, to a lesser extent, of L293 in the first P-loop affected both the high- and low-affinity characteristics in concert, suggesting an overlap in the structural features underlying the two separate K^+-sensitivities.

In the present study, we found that both N275D and N410D mutation affected the slowest relaxations, increasing the amplitude of the slow component of activation and affecting the time constant for the slow component of deactivation (Figs. 1–3). The effects of the mutations were evident at sub-millimolar $[K^+]_o$. These characteristics are consistent with alterations to the $C_4 \leftrightharpoons C_3$ transition, favouring the more distal C_4 state in low $[K^+]_o$. Significantly, the mutations did not affect the actions of high $[K^+]_o$ on the current associated with the $C_3 \leftrightharpoons C_2$ transitions proximal to the open state. Neither mutation influenced the voltage-dependence of the steady-state conductance nor its alkali cation-selectivity (Figs. 4 and 5). The observations, thus, add strength to the argument for two physically distinct K^+ binding sites with differing affinities for the cation [11], only one of which is affected by mutation at residues N275 and N410.

Differences in the kinetic characteristics introduced by the mutations also suggest that the two pore domains do not contribute equally to YKC1 gating. Although both mutants affected the slow component of activation and deactivation, they differed substantially in their actions on the $[K^+]_o$-sensitivities of the component current amplitudes and relaxations (see Figs. 2 and 3). The N410D mutant increased the apparent $K_{1/2}$ for K^+ action on the current components during activation, but its influence on relaxations between distal channel states following negative voltage steps was purely scalar, without significant effect on the $[K^+]_o$-sensitivity. By contrast, the N275D mutant had a profound effect on the $[K^+]_o$-sensitivity evident on deactivating voltage steps, but was largely without action on the $[K^+]_o$-sensitivity evident from activating voltage steps. The contrasting actions of the mutations can be accommodated if the transition between C_4 and C_3 subsumes an additional state following K^+ binding in the forward direction and, hence, kinetically separates the actions of the two mutations. The importance of this separation is highlighted by the double N410D-N275D mutant (Figs. 2 and 3) that showed alterations in the apparent affinities for external K^+ that matched each of the single mutants, that is the $[K^+]_o$-sensitivity of N410D for current activation and the loss of $[K^+]_o$-sensitivity of N275D for current deactivation. Thus, unlike C-type inactivation of Shaker K^+ channel pore [24–26], the two YKC1 P-loops clearly do not contribute equally to channel gating.

What structures are associated with the mutated asparagines? Based on sequence homology to the *Streptomyces* KcsA K^+ channel, residues N275 and N410 in YKC1 are probably situated alternately, one in each of the 'turrets' and are exposed to the aqueous phase on the outer surface of the membrane [13,27]. Thus, two of the four turrets are predicted each to contain a N275 residue and the other two a N410 residue, consistent with the 2-fold symmetry of a channel comprised of two homologous monomers each with two P-loops [9,28]. Both residues are probably situated sufficiently close to residues in the outer mouth of the pore to interact in the gating process. Within each P-loop of the KcsA channel, arginine 64 (corresponding to N275 and N410 of YKC1) is predicted to lie within 8–11 Å of tyrosine 82 (corresponding to L293 and A428) in the extracellular loop immediately following the K^+-selectivity filter. By contrast, the distances of corresponding residues across P-loop boundaries of the KcsA channel are greater (11–15 Å). These distances are somewhat greater than might be expected for a single site coordinating an alkali cation, but nonetheless could be close enough for electrostatic interactions to alter the energy landscape of a nearby cation binding site. The fact that the double mutants

N275D-A428Y and N410D-A428Y did not express measurable currents whereas the single mutants do (see also [11]) suggests that some interactions between mutations at the C- and N-termini of the P-loops do take place.

In fact, a degree of interaction might well be anticipated, based on parallels with the Shaker K^+ channel. Like T449 of the Shaker K^+ channel, L293 and A428 of YKC1 probably protrude into the outer vestibule of the pore immediately outside the entry to the K^+-selectivity filter [13] and form part of an external gate [24,26]. Significantly, C-type inactivation of the Shaker K^+ channel is affected both by external K^+ and binding of the K^+ channel blocker TEA [29]. Residues N275 and N410 of YKC1 correspond to D431 of the Shaker K^+ channel that, like T449, contributes to scorpion toxin and TEA binding outside [14–16,29]. So, N275 and N410 may well define points of interaction with L293 and A428 at the opposite end of the P-loops.

In conclusion, we have explored mutations at equivalent residues N-terminal from the K^+ channel signature sequences in each of the YKC1 P-loops. Substitutions of the asparagines with aspartate residues at either or both of these sites influenced kinetic characteristics that were previously associated with a high-affinity, regulatory K^+ binding site. Gating characteristics previously associated with low-affinity K^+ binding were unaffected, thereby supporting the idea of two physically distinct binding sites. Both quantitative and qualitative differences between channels with one or the other of the asparagines mutated indicate a divergence in gating functions for the two P-domains of the YKC1 K^+ channel and echo functional differences between domains recently uncovered in the gating of the human skeletal muscle Na^+ channel [30].

Acknowledgements: We thank Alexander Grabov for comments on the manuscript. P.V. was supported by Grant C07797 from the British Biotechnology and Biological Sciences Research Council.

References

[1] Bertl, A., Slayman, C.L. and Gradmann, D. (1993) J. Membr. Biol. 132, 183–199.
[2] Lesage, F., Guillemare, E., Fink, M., Duprat, F., Lazdunski, M., Romey, G. and Barhanin, J. (1996) J. Biol. Chem. 271, 4183–4187.
[3] Blatt, M.R. and Gradmann, D. (1997) J. Membr. Biol. 158, 241–256.
[4] Thiel, G. and Wolf, A.H. (1997) Trends Plant Sci. 2, 339–345.
[5] Miosga, T., Witzel, A. and Zimmermann, F.K. (1994) Yeast 10, 965–973.
[6] Ketchum, K.A., Joiner, W.J., Sellers, A.J., Kaczmarek, L.K. and Goldstein, S.A.N. (1995) Nature 376, 690–695.
[7] Reid, J.D., Lukas, W., Shafaatian, R., Bertl, A., Scheurmann-kettner, C., Guy, H.R. and North, R.A. (1996) Recept. Channels 4, 51–62.
[8] Vergani, P., Miosga, T., Jarvis, S.M. and Blatt, M.R. (1997) FEBS Lett. 405, 337–344.
[9] Goldstein, S.A.N. (1996) Neuron 16, 717–722.
[10] Jan, L.Y. and Jan, Y.N. (1994) Nature 371, 119–122.
[11] Vergani, P., Hamilton, D., Jarvis, S. and Blatt, M.R. (1998) EMBO J. 17, 7190–7198.
[12] Lopez-Barneo, J., Hoshi, T., Heinemann, S.H. and Aldrich, R.W. (1993) Recept. Channels 1, 61–71.
[13] Doyle, D.A., Cabral, J.M., Pfuetzner, R.A., Kuo, A.L., Gulbis, J.M., Cohen, S.L., Chait, B.T. and MacKinnon, R. (1998) Science 280, 69–77.
[14] Goldstein, S.A.N., Pheasant, D.J. and Miller, C. (1994) Neuron 12, 1377–1388.
[15] Yellen, G., Jurman, M.E., Abramson, T. and MacKinnon, R. (1991) Science 251, 939–942.
[16] MacKinnon, R., Heginbotham, L. and Abramson, T. (1990) Neuron 5, 767–771.
[17] Groves, J.D. and Tanner, M.J.A. (1992) J. Biol. Chem. 267, 22163–22170.
[18] Ray, F.A. and Nickoloff, J.A. (1992) Biotechniques 13, 342–344.
[19] Higuchi, R. (1990) in: Recombinant PCR (Innis, M.A., Gelfand, D.H., Sninsky, J.J. and White, T.J., Eds.), pp. 177–196.
[20] Press, W., Flannerly, B., Teukolsky, S. and Vetterling, W. (1986) Numerical Recipies: The Art of Scientific Computing, Cambridge University Press, Cambridge.
[21] Loukin, S.H., Vaillant, B., Zhou, X.L., Spalding, E.P., Kung, C. and Saimi, Y. (1997) EMBO J. 16, 4817–4825.
[22] Zhou, X.L., Vaillant, B., Loukin, S.H., Kung, C. and Saimi, Y. (1995) FEBS Lett. 373, 170–176.
[23] Blatt, M.R. (1991) J. Membr. Biol. 124, 95–112.
[24] Liu, Y., Jurman, M.E. and Yellen, G. (1996) Neuron 16, 859–867.
[25] Yellen, G., Sodickson, D., Chen, T.-Y. and Jurman, M.E. (1994) Biophys. J. 66, 1068–1075.
[26] Ogielska, E.M., Zagotta, W.N., Hoshi, T., Heinemann, S.H., Haab, J. and Aldrich, R.W. (1995) Biophys. J. 69, 2449–2457.
[27] Sun, Z.P., Akabas, M.H., Goulding, E.H., Karlin, A. and Siegelbaum, S.A. (1996) Neuron 16, 141–149.
[28] MacKinnon, R. (1995) Neuron 14, 889–892.
[29] Choi, K.L., Aldrich, R.W. and Yellen, G. (1991) Proc. Nat. Acad. Sci. USA 88, 5092–5095.
[30] Cha, A., Ruben, P.C., George, A.L., Fujimoto, E. and Bezanilla, F. (1999) Neuron 22, 73–87.